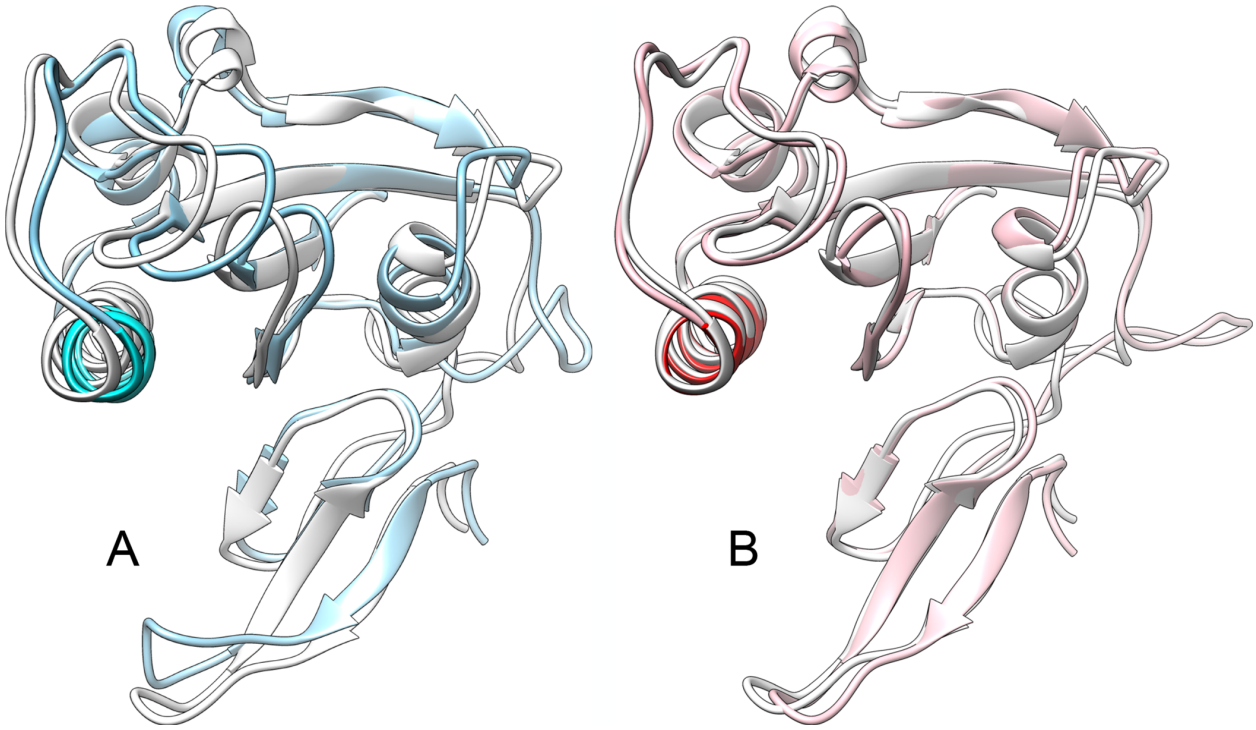

Figure S1, related to Figure 2. The positioning of α1 relative to the PPIase core and the WW domain

(A) Relative to apo Pin1 (gray), α1 (darker cyan) moves closer to the other two modules (cyan) upon binding FFpSPR.

(B) In the simulation with the interface(Pin1) restraints, α1 (red) stays in the same position as in the unrestrained apo Pin1 simulation (gray).

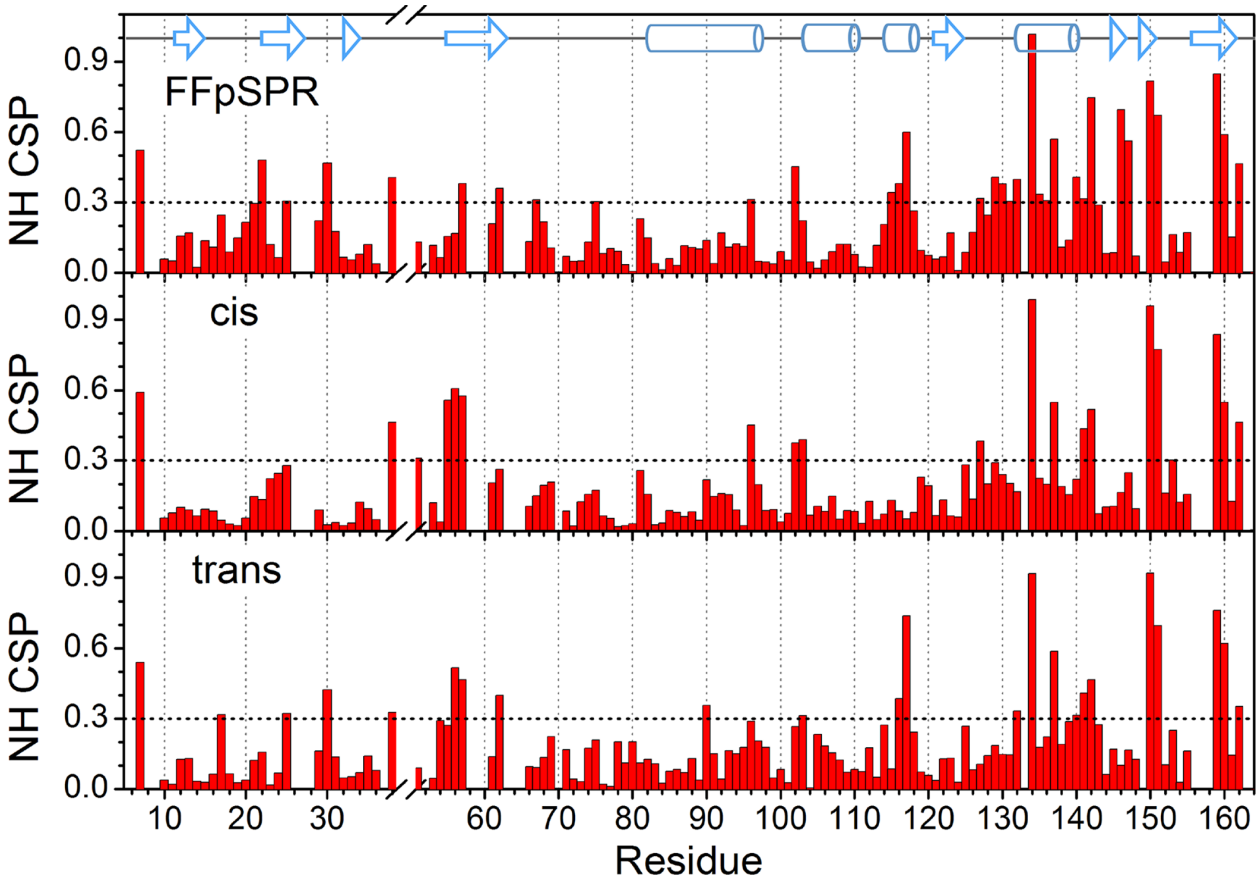

Figure S2, related to Figure 2. NH chemical shift perturbations (CSPs) of Pin1 upon binding of the three ligands, from backbone chemical shifts predicted by SPARTA+ on our simulations of the four systems

The N and H chemical shifts of the apo form are subtracted from those of each ligand-bound form.

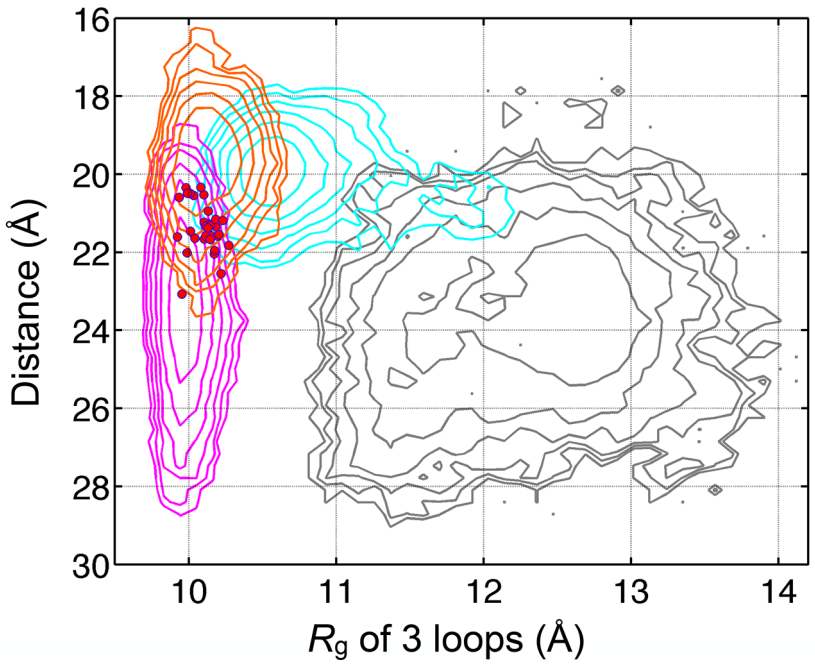

Figure S3, related to Figure 2. Overlaid free energy surfaces of four systems over two collective coordinates

The first coordinate is the radius of gyration (R_g) of the three catalytic-site loops (residues 63-72, 126-132, and 151-155); the second coordinate is the distance between the centers of Cα atoms in the β1-β2 loop (residues 15-21) and the α1 helix (residues 82-97). Results for the four systems are shown in different colors: gray for apo Pin1; and cyan, orange, and magenta for the FFpSPR-, *trans* ligand-, and *cis* ligand-bound forms, respectively. The coordinates of the 32 crystal structures are shown as red dots.

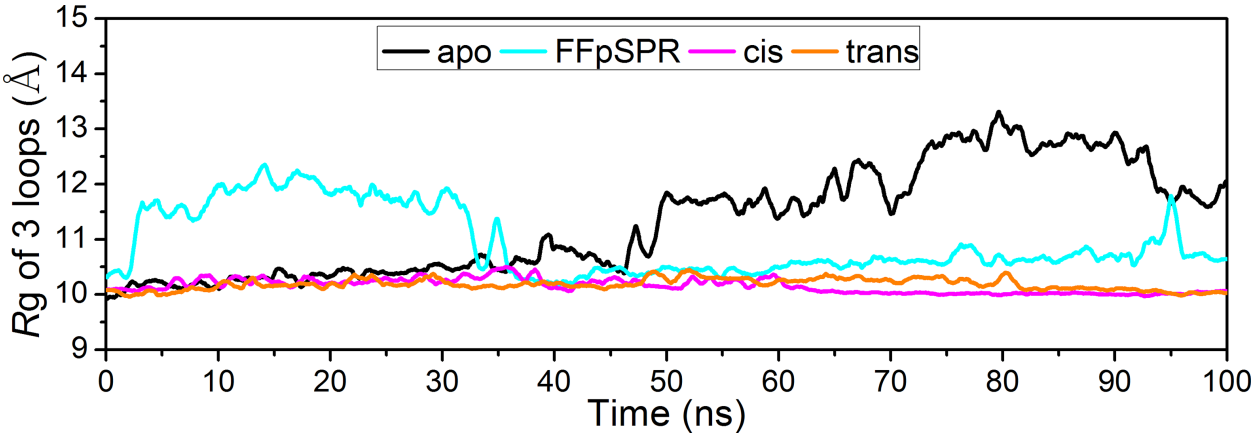

Figure S4, related to Figure 3. R_g of the three catalytic-site loops during the full 100-ns simulations of the four systems

The data are smoothed over a 1-ns window.

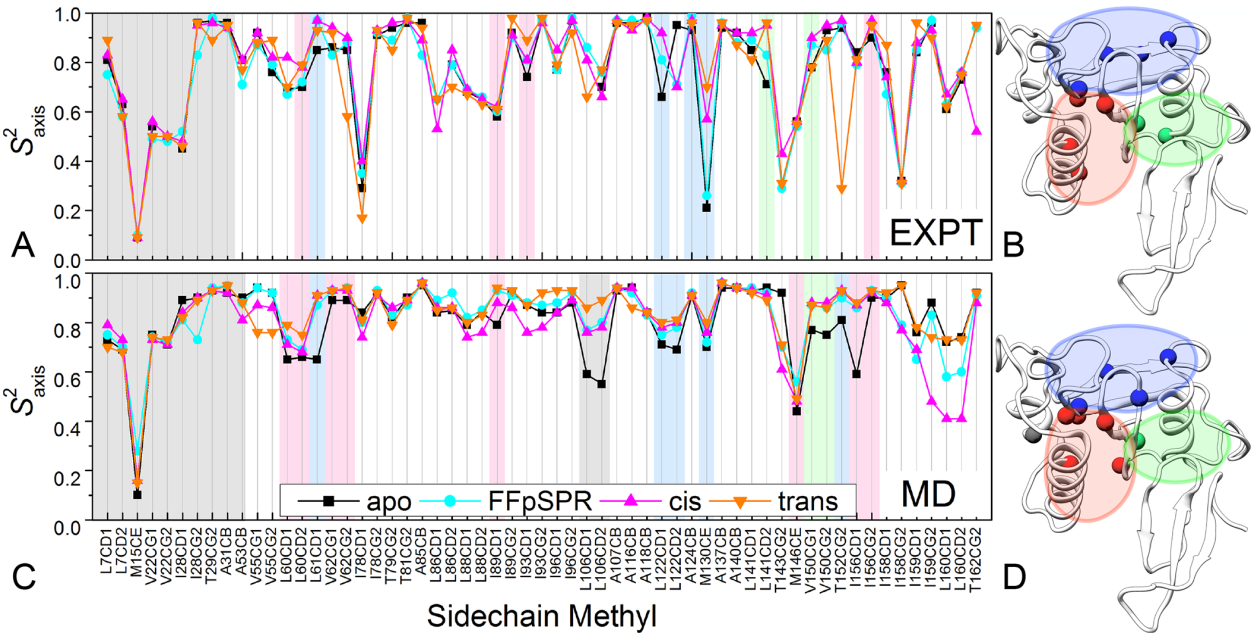

Figure S5, related to Figure 3. Order parameters (S^2_{axis}) of sidechain methyls from NMR experiments (Namanja et al., 2011) and our simulations

(A) NMR S^2_{axis}, with those increasing upon ligand binding highlighted by blue, red, and green shading.

(B) The residues highlighted in blue, red, and green are shown to fall into the catalytic site, the α1-PPIase core interface, and the PPIase-WW interface, respectively.

(C,D) Corresponding results from the simulations.

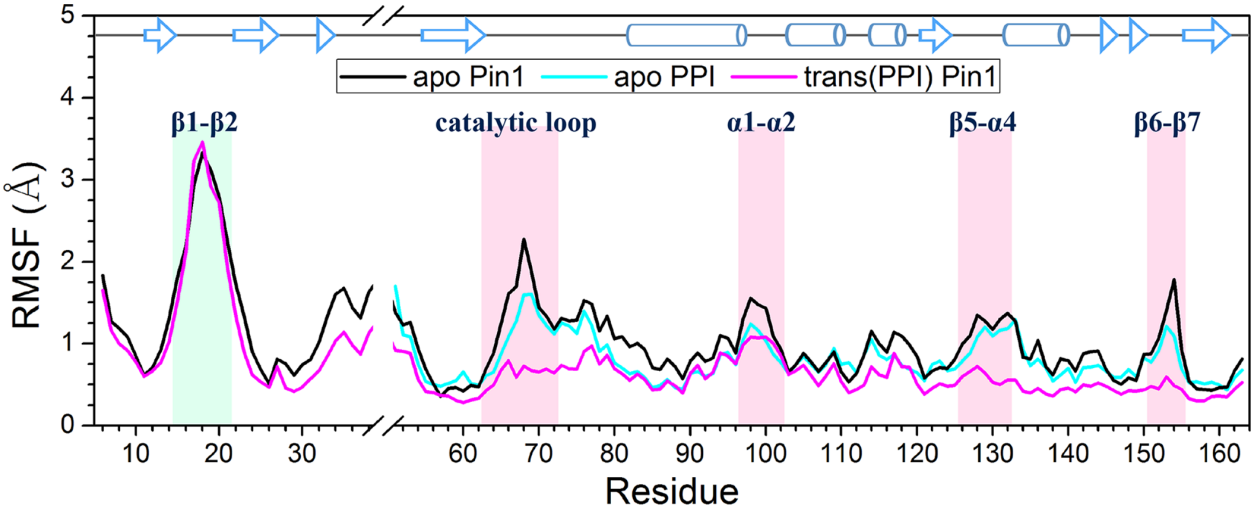

Figure S6, related to Figure 3. The Cα root-mean-square-fluctuations (RMSFs) of the isolated PPIase domain in apo form and of full-length Pin1 with a *trans* ligand bound only at the catalytic site, compared to the results for apo Pin1

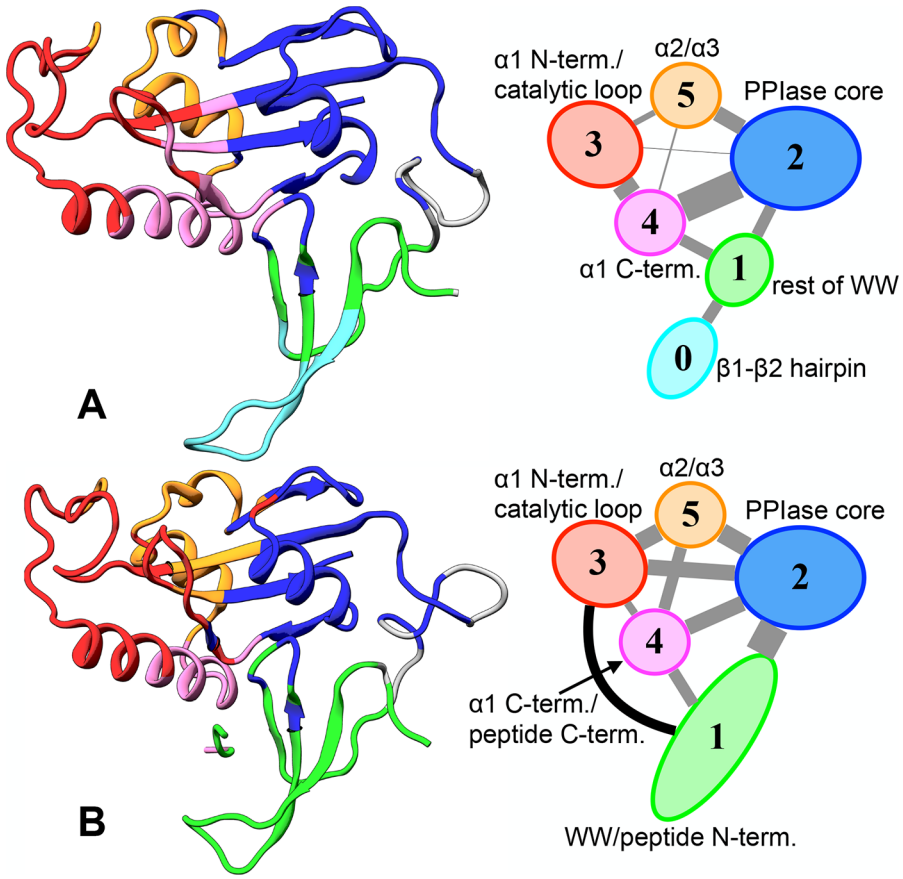

Figure S7, related to Figure 4. Community analysis results

(A) Apo form.

(B) With FFpSPR bound at the WW site.

The communities are shown in different colors as cartoon structures (left) or as circles (right). Inter-community connections are shown as lines, with width proportional to the cumulative betweenness. The community network analysis was performed using the NetworkView plugin in VMD with default setting.

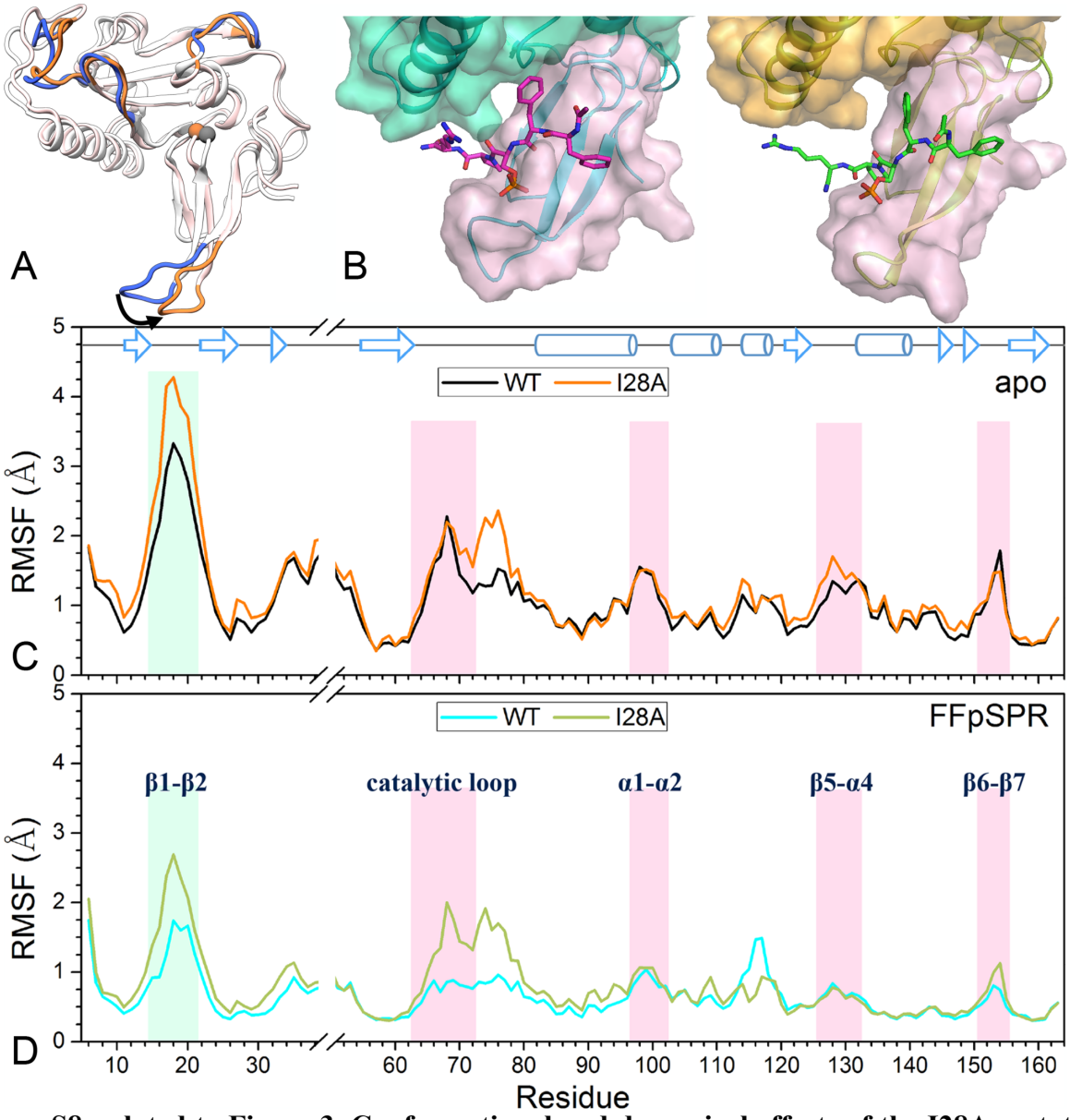

Figure S8, related to Figure 3. Conformational and dynamical effects of the I28A mutation on apo and FFpSPR-bound Pin1

(A) Comparison of average conformations between wild-type (WT; gray with four blue loops) and mutant (pink with four orange loops) apo Pin1. The Cα atom of the residue undergoing mutation is shown as a sphere (gray for wild-type and orange for mutant). Significant opening of the β1-β2 loop upon mutation is indicated by an arrow.

(B) Average conformations of the FFpSPR-Pin1 complex before (*left*) and after (*right*) the mutation.

(C,D) Cα RMSFs of mutated Pin1 in apo and FFpSPR-bound forms, compared to the WT results.

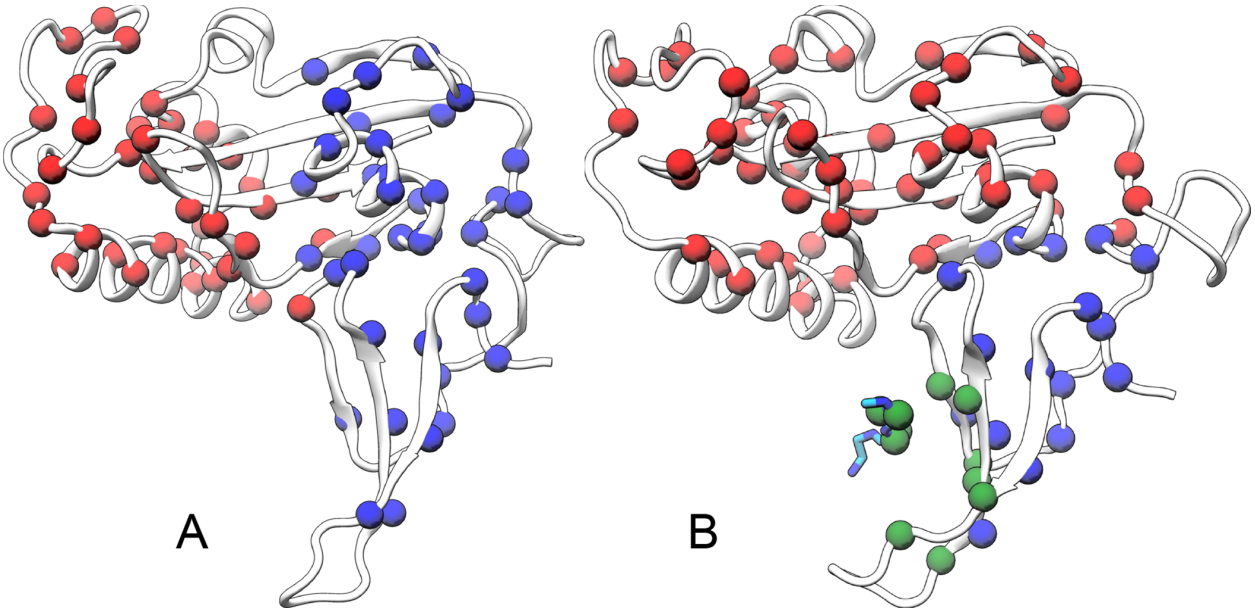

Figure S9, related to Figure 4. Allosteric networks of the I28A mutant

(A) Apo form.

(B) With FFpSPR bound at the WW site.

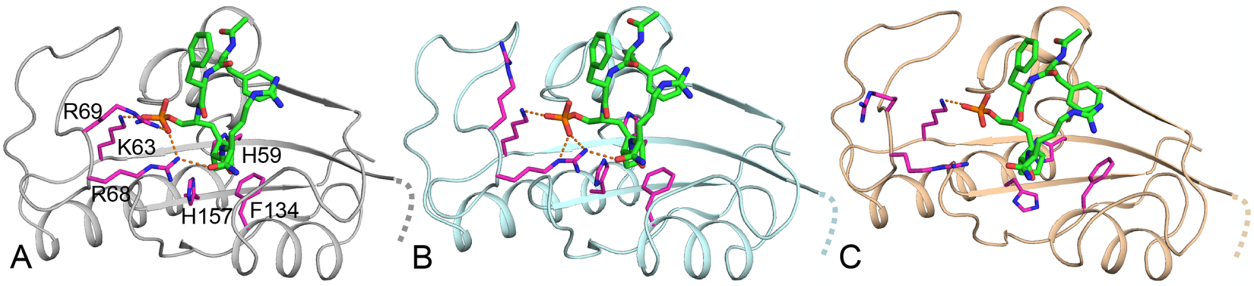

Figure S10, related to Figure 6. Docked poses for the *cis* ligand at the catalytic site, generated using RosettaLigand on conformations from our simulations

(A) The optimal pose of the ligand, refined from the simulation of Pin1 with this ligand bound at the catalytic site. The ligand Pro residue is properly positioned relative to Pin1 His59, Phe134, and His157; the ligand pSer sidechain forms salt bridges with Lys63, Arg68, and Arg69 of the catalytic loop.

(B) The ligand docked to the empty catalytic site of a conformation from the simulation of Pin1 with FFpSPR bound at the WW site. The ligand Pro residue is also properly positioned, and the pSer sidechain still forms some of the salt bridges in (A).

(C) The ligand docked to the catalytic site of a conformation from the simulation of apo Pin1. As the Pin1 His59, Phe134, and His157 rings are misoriented, the ligand Pro residue sinks too deeply into the binding pocket. The ligand-Pin1 interaction energies obtained for the three systems are -14.3 ± 0.6, -11.5 ± 1.3, and -7.3 ± 1.2 kcal/mol, respectively.